Matrix method to predict the spectral reflectance of stratified surfaces including thick layers and thin films

Mathieu Hébert, Lionel Simonot, Serge Mazauric

Matrix method to predict the spectral reflectance of stratified surfaces including thick layers and thin films

Mathieu Hébert[1], Lionel Simonot[2], Serge Mazauric[3]

[1]Université de Lyon, Université Jean Monnet de Saint-Etienne, CNRS, Institut d'Optique Graduate-School, UMR 5516 Laboratoire Hubert Curien, F-42000 Saint-Etienne, France.

[2] Université de Poitiers, CNRS UPR 3346 Institut Pprime, 11 Boulevard Marie et Pierre Curie, BP 30179, F-86962 Futuroscope Chasseneuil Cedex, France.

[3] CPE-Lyon, Domaine Scientifique de la Doua, 43 boulevard du 11 Novembre 1918 BP 82077, 69616 Villeurbanne Cedex, France.

1. Abstract

The most convenient way to assess the color rendering of a coated, painted, or printed surface in various illumination and observation configurations is predict its spectral, angular reflectance using an optical model. Most of the time, such a surface is a stack of layers having different scattering properties and different refractive indices. A general model applicable to the widest range of stratified surfaces is therefore appreciable. This is what we propose in this paper by introducing a method based on light transfer matrices: the transfer matrix representing the stratified surface is the product of the transfer matrices representing the different layers and interfaces composing it, each transfer matrix being expressed in terms of light transfers (e.g. diffuse reflectances and transmittances in the case of diffusing layers). This general model, inspired of models used in the domain of thin films, can be used with stacks of diffusing or nonscattering layers for any illumination-observation geometry. It can be seen, in the case of diffusing layers, as an extension of the Saunderson-corrected Kubelka-Munk model and Kubelka's layering model. We illustrate the through an experimental example including a thin coating, a thick glass plate and a diffusing background.

2. Introduction

For a long time, the variation of the spectral properties of surfaces and objects by application of coatings has been a wide subject of investigation for physicians who proposed several models based on specific mathematical formalisms according to the type of physical components and the application domain. In the domain of paints, papers, and other diffusing media, a classical approach is to use the Kubelka-Munk system of two coupled differential equations to describe the propagation of diffuse fluxes in the medium [1,2]. The extension of this model by Kubelka to stacks of paint layers is based on geometrical series describing the multiple reflections and transmissions of these diffuse fluxes between the different layers [3,4]. Geometrical series were also used by Saunderson [5] when deriving his correction of the Kubelka-Munk model in order to account for the internal reflections of light between the paint layer and the paint-air interface, by Clapper and Yule [6] in their reflectance model

for halftone prints to account for the internal reflections of light between the paper and the print-air interface across the inks, and by Williams and Clapper [7] in their model for gelatin photograph to account for the internal reflections of light between the paper and the print-air interface across the nonscattering gelatin layer. More recently, alternative mathematical methods using graphs [8], Markov chains [9] or continuous fractions [10,11] were proposed to derive the equations of these models in a more efficient way, especially when their structure or the number of layer increases. In the domain of thin coatings, the models are rather based on the multiple reflections of coherent optical waves generating interferences at normal or near-normal incidence [13]. Despite their apparent dissimilarity, all these models have in common to be comparable to a two-flux model describing the mutual exchanges between downward and upward propagating light quantities, by reflection or transmission of light by the different layers and surfaces. In the case of weakly scattering media, e.g. pigmented media [14,15], advanced models based on the radiative transfer theory [16] or on multi-flux approaches [17] are needed to take into account more thoroughly the orientations of scattered light. However, in all the previously cited configurations where the media are either very scattering or almost non-scattering, the two-flux-like approach generally provides good prediction accuracy and the equations can be turned into vector equations involving 2×2 transfer matrices. This matrix formalism is well known in the case of thin films illuminated a normal incidence by coherent light modeled by complex amplitudes of electromagnetic fields [18], or in the case of diffusing layers illuminated by diffuse incoherent fluxes [19], but it is less known that similar formalism actually applies to any stack of thin layers, thick nonscattering layers, and/or diffusing layers, provided appropriate light models (complex amplitude of waves, oriented collimated fluxes or diffuse fluxes) are used for each type of layer. However, the reflectance and transmittance of a thin layer computed by considering coherent, directional light can be combined with the reflectance and transmittance of a thick nonscattering layer by considering directional, directional light, then with the reflectance and transmittance of a thick layer by considering Lambertian flux. Some objects containing thin, thick and diffusing layers are well known, e.g. luster ceramics which display an angle-dependent colored sheen in addition to their ground color due to the fact that a thin absorbing layer made by metallic nanoparticles is embedded in the thick nonscattering glaze layer covering the diffusing ceramics background [20]. In the domain of color reproduction, similar structure can be found in colored samples produced by new ink-less printing technologies, e.g. the technology presented in Ref. [21] where thin layers of silver nanoparticles in a titanium oxide matrix with photochromics properties are deposited on a clear support (e.g. glass or polymer) or a diffusing support (pigmented polymer or paper). Since a printing technology aims at producing many samples with different colors on different supports, a model able to predict easily the color rendering of all of them for any illumination-observation geometry might be appreciable. In comparison to more classical mathematical methods, the matrix method that we propose may considerably ease the derivation of analytical expressions for reflectance and transmittance of the specimens and enables fast numerical computation.

This paper aims at presenting the matrix method in a general way, before showing how to use it in different contexts. We will first present the matrix method by using a generic terminology standing for complex amplitude of waves as well as for fluxes of photons: we will call "transfer" the reflection or

transmission of propagating optical quantity, and "transfer factor" a fraction of quantity which is transferred. According to the direction of the incoming quantity and according to whether the transfer is due to reflection or transmission, four transfer factors can be distinguished: front and back reflection factors, and forward and backward transmission factors. After this general presentation (Section 3), we propose to deal specifically with diffusing layers (Section 4), nonscattering layers (Section 4) and thin coatings (Section 5). Section 7 briefly explains the methodology to follow when these different kinds of layers are stacked with each other, a methodology which is illustrated in detail in Section 8 through the example of glass plates coated with thin silicon deposits and placed in front of a white diffusing background.

3. General model

Let us consider planar optical components labeled by increasing number k from front to back. The light quantities propagating forwards are denoted I_k and those propagating backwards J_k, where k indicates the position in the stack of components (see Figure 1). The light transfers in component k due to reflections are quantified by transfer factors denoted r_k (front-side reflection) and r'_k (back-side reflection); those due to transmissions through component k are denoted t_k (forward transmission), and t'_k (backward transmission).

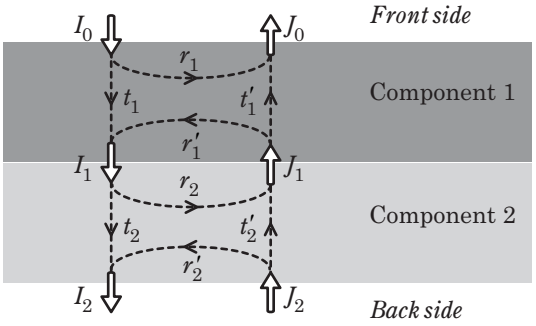

Figure 1: Transfers between two flat optical components (the arrows do not render the orientation of light).

In each component k, one can write the following relations between incoming and outgoing quantities

$$\begin{aligned} J_{k-1} &= r_k I_{k-1} + t'_k J_k, \\ I_k &= t_k I_{k-1} + r'_k J_k, \end{aligned} \tag{1}$$

and turn them into the following vector equation

$$\begin{pmatrix} -r_k & 1 \\ t_k & 0 \end{pmatrix} \begin{pmatrix} I_{k-1} \\ J_{k-1} \end{pmatrix} = \begin{pmatrix} 0 & t'_k \\ 1 & -r'_k \end{pmatrix} \begin{pmatrix} I_k \\ J_k \end{pmatrix}, \tag{2}$$

or, assuming $t_k \neq 0$, into the following one:

$$\begin{pmatrix} I_{k-1} \\ J_{k-1} \end{pmatrix} = \mathbf{M}_k \begin{pmatrix} I_k \\ J_k \end{pmatrix} \tag{3}$$

where $\mathbf{M}_k$ is the transfer matrix representing component k:

$$\mathbf{M}_k = \frac{1}{t_k}\begin{pmatrix} 1 & -r'_k \\ r_k & t_k t'_k - r_k r'_k \end{pmatrix} \tag{4}$$

Regarding the two components 1 and 2 together, Eq. (3) can be repeated twice and one gets:

$$\begin{pmatrix} I_0 \\ J_0 \end{pmatrix} = \mathbf{M}_1 \begin{pmatrix} I_1 \\ J_1 \end{pmatrix} = \mathbf{M}_1 \cdot \mathbf{M}_2 \begin{pmatrix} I_2 \\ J_2 \end{pmatrix} = \mathbf{M}_{12} \begin{pmatrix} I_2 \\ J_2 \end{pmatrix} \tag{5}$$

where $\mathbf{M}_{12}$ is the transfer matrix representing the two layers together, similarly defined as Eq. (4) in terms of its transfer factors r_{12}, t_{12}, r'_{12} and t'_{12}.

Eq. (5) shows that the transfer matrix representing two superposed components is the product of the component's individual transfer matrices. The multiplicativity of transfer matrices is true for any number of components, and the left-to-right position of the matrices in the product reproduces the front-to-back position of the corresponding components. Every transfer matrix in this model has the structure displayed in Eq. (4) and from a given transfer matrix $\mathbf{M} = \{m_{ij}\}$, one retrieves the transfer factors r, r', t and t' in the following way:

$$r = m_{21} / m_{11}, \tag{6}$$

$$t = 1 / m_{11}, \tag{7}$$

$$r' = -m_{12} / m_{11}, \tag{8}$$

and

$$t' = m_{22} - m_{21} m_{12} / m_{11}. \tag{9}$$

It is important to notice that the forward transmission factor may be zero, in particular each time an oblique radiance strikes a flat interface beyond the critical angle. The transfer matrix defined by (4) thus becomes indefinite. Although, in sake of clarity, we will continue to use this definition for the transfer matrices in the following, we recommend using an alternative definition of the transfer matrices for numerical computation:

$$\mathbf{M}_k = \begin{pmatrix} 1 & -r'_k & 0 \\ r_k & t_k t'_k - r_k r'_k & 0 \\ 0 & 0 & \tau_k \end{pmatrix} \tag{10}$$

From a transfer matrix $\mathbf{M} = \{m_{ij}\}$ defined by Eq. (10), the transfer factors r, r' and t' are still given by the formulas (6), (8) and (9), respectively, and the transfer factor t is given by m_{33} / m_{11}.

Let us come back to case of two components represented by the matrices $\mathbf{M}_1$ and $\mathbf{M}_2$ defined by Eq. (4). From the matrix $\mathbf{M}_{12} = \mathbf{M}_1 \cdot \mathbf{M}_2$ representing the two components together, using the formulas (6) to (9), one obtains the following transfer factors:

$$\begin{aligned} r_{12} &= r_1 + \frac{t_1 t'_1 r_2}{1 - r'_1 r_2}, \quad & t_{12} &= \frac{t_1 t_2}{1 - r'_1 r_2}, \\ r'_{12} &= r'_2 + \frac{t_2 t'_2 r'_1}{1 - r'_1 r_2}, \quad & t'_{12} &= \frac{t'_1 t'_2}{1 - r'_1 r_2}. \end{aligned} \tag{11}$$

The expressions for the transfer factors become more complex as the number of stacked components increases, except in the case where all the components are identical (see for example an application based on stacked of printed films in Ref [11] or duplex halftone prints in Ref. [12]). In this case, there

is an interest in diagonalizing the matrix **M** representing each component, defined as in Eq. (10) in terms of the transfer factors r, r', t and t'. Using the notations

$$a = \frac{1 + rr' - tt'}{2\sqrt{rr'}}, \tag{12}$$

$$b = \sqrt{a^2 - 1}, \tag{13}$$

and

$$\mathbf{E} = \begin{pmatrix} a-b & a+b \\ 1 & 1 \end{pmatrix}, \tag{14}$$

M can be decomposed as

$$\mathbf{M} = \frac{1}{t}\mathbf{E} \cdot \begin{pmatrix} 1-(a+b)\sqrt{rr'} & 0 \\ 0 & 1-(a-b)\sqrt{rr'} \end{pmatrix} \cdot \mathbf{E}^{-1} \tag{15}$$

and the transfer matrix representing the stack of N identical components is:

$$\mathbf{M}^N = \frac{1}{t^N}\mathbf{E} \cdot \begin{pmatrix} \left(1-(a+b)\sqrt{rr'}\right)^N & 0 \\ 0 & \left(1-(a-b)\sqrt{rr'}\right)^N \end{pmatrix} \cdot \mathbf{E}^{-1} \tag{16}$$

After computing this matrix and using formulas (6) to (9), one obtains respectively:

$$r_N = \left[a - b\left(1 - \frac{2}{1 - \left[\frac{1-(a+b)\sqrt{rr'}}{1-(a-b)\sqrt{rr'}} \right]^N} \right) \right]^{-1}, \tag{17}$$

$$t_N = \frac{2bt^N}{(a+b)\left[1-(a-b)\sqrt{rr'}\right]^N - (a-b)\left[1-(a+b)\sqrt{rr'}\right]^N}, \tag{18}$$

$$r'_N = r_N r'/r, \tag{19}$$

and

$$t'_N = t_N \left(t'/t\right)^N. \tag{20}$$

As N increases to infinity, the reflection factor r_N tends to the limit factor:

$$r_\infty = \frac{\sqrt{r/r'}}{a+b} = (a-b)\sqrt{r/r'} \tag{21}$$

Note that all light quantities and transfer factors in this model may depend upon wavelength, polarization and orientation of light.

4. Case of diffusing layers

It is known that the reflection and transmission of light by strongly diffusing layers can be modeled according to a two flux approach [22, 3, 4], thereby by the present matrix model. In this case, the quantities I and J are Lambertian fluxes and the transfer factors are the layers' diffuse reflectances and transmittances. Eqs. (11) are equivalent to those presented by Kubelka in Ref. [3]. In the special case where the layers are made of same medium, the Kubelka-Munk model applies [1, 2] and the matrix

model enables retrieving the Kubelka-Munk reflectance and transmittance formulas, as shown in Ref. [10] with a matrix formalism similar to the present one. We propose to show it in a slightly different way, by using Eqs. (17) and (18).

Let us consider a layer of thickness h with reflectance ρ and transmittance τ and subdivide it into n identical sublayers with reflectances and transmittances denoted $\rho_{h/n}$ and $\tau_{h/n}$. Since we have a stack of identical components, we can use Formulas (17) and (18). As n tends to infinity, the reflectance of one sublayer is the fraction of backscattered light which is, according to the Kubelka-Munk, proportional to the diffuse backscattering coefficient S and the thickness of the layer:

$$\rho_{h/n} = S\frac{h}{n} \tag{22}$$

The transmittance of the sublayer is the amount of light which is not absorbed and not scattered, i.e.

$$\tau_{h/n} = 1-(K+S)\frac{h}{n} \tag{23}$$

where K denotes the diffuse absorption coefficient. Parameters a and b defined by Eqs. (12) and (13) become:

$$a = \lim_{n\to\infty}\frac{1+\rho_{h/n}^2-\tau_{h/n}^2}{2\rho_{h/n}} = \frac{K+S}{S}, \tag{24}$$

and

$$b = \sqrt{a^2-1}\,, \tag{25}$$

and using a classical result for the exponential function [23]

$$\lim_{N\to\infty}\left(1+\frac{x}{N}\right)^N = e^x\,, \tag{26}$$

one can write:

$$\lim_{n\to\infty}\frac{\left[1-(a+b)\frac{Sh}{n}\right]^n}{\left[1-(a-b)\frac{Sh}{n}\right]^n} = \frac{e^{-(a+b)Sh}}{e^{-(a-b)Sh}} = e^{-2bSh}, \tag{27}$$

Formulas (17) and (18) thus become:

$$\rho_h = \left[a-b\left(1-\frac{2}{1-e^{-2bSh}}\right)\right]^{-1} = \frac{1}{a+b\coth(bSh)} \tag{28}$$

and

$$\tau_h = \frac{2be^{-aSh}}{(a+b)e^{-(a-b)Sh}-(a-b)e^{-(a+b)Sh}} = \frac{b}{a\sinh(bSh)+b\cosh(bSh)} \tag{29}$$

which are the Kubelka-Munk reflectance, respectively transmittance expressions, identical at the front and back sides. The transfer matrix representing the diffusing layer is:

$$\mathbf{M} = \frac{1}{\tau_h}\begin{pmatrix} 1 & -\rho_h \\ \rho_h & \tau_h^2-\rho_h^2 \end{pmatrix} \tag{30}$$

Most of the time, the layer has a different refractive index as the surrounding medium (e.g. air). In this case, the reflections and transmissions of light by the interfaces have a non-negligible effect that must been taken into account. Saunderson [5] proposed a reflectance formula correcting the Kubelka-Munk reflectance expression by considering one interface at the front side (the layer being assumed bordered by a medium of same index at the back side). Here, we propose to consider that the medium is surrounded by air (medium 0) at both sides.

By denoting $R_{01}(\theta)$ the angular reflectance of the air-medium interface at the air side, given by Fresnel's formulas, one obtains the diffuse reflectance of the interface (for Lambertian illumination at the air side) by integrating the angular reflectance over the hemisphere [24]:

$$\tilde{R}_{01} = \int_{\theta=0}^{\pi/2} R_{01}(\theta)\sin(2\theta)d\theta \tag{31}$$

The diffuse transmittance from air to the medium is $\tilde{T}_{01} = 1 - \tilde{R}_{01}$, the diffuse reflectance at the medium side is $\tilde{R}'_{01} = 1 - (1 - \tilde{R}_{01})/n^2$ and the diffuse transmittance from the medium to air is $\tilde{T}'_{01} = \tilde{T}_{01}/n^2$, where n is the refractive index of the medium [8]. The transfer matrix representing the interface at the front and back sides are respectively

$$\tilde{\mathbf{F}}_{01} = \frac{1}{\tilde{T}_{01}}\begin{pmatrix} 1 & -\tilde{R}'_{01} \\ \tilde{R}_{01} & \tilde{T}_{01}\tilde{T}'_{01} - \tilde{R}_{01}\tilde{R}'_{01} \end{pmatrix}, \tag{32}$$

and

$$\tilde{\mathbf{F}}_{10} = \frac{1}{\tilde{T}'_{01}}\begin{pmatrix} 1 & -\tilde{R}_{01} \\ \tilde{R}'_{01} & \tilde{T}_{01}\tilde{T}'_{01} - \tilde{R}_{01}\tilde{R}'_{01} \end{pmatrix}. \tag{33}$$

They only depend on the refractive index of the medium. The transfer matrix representing the layer with interfaces is:

$$\mathbf{M}_S = \tilde{\mathbf{F}}_{01} \cdot \mathbf{M} \cdot \tilde{\mathbf{F}}_{10} \tag{34}$$

with $\mathbf{M}$ given by Eq. (30). By computing the matrix $\mathbf{M}_S$ and using formula (6), one obtains the reflectance and transmittance ρ_S and τ_S of the layer with interfaces, identical at both sides due to the fact that the layer is symmetrical and illuminated by Lambertian fluxes at both sides. Note that $\mathbf{M}$ and $\mathbf{M}_S$ may be spectral matrices, i.e. they are evaluated for each waveband of the considered spectrum.

In practice, ρ_S and τ_S may be measured using a spectro-photometer (in diffuse:diffuse geometry), and the matrix representing the layer with interfaces can be defined for each waveband:

$$\mathbf{M}_S = \frac{1}{\tau_S}\begin{pmatrix} 1 & -\rho_S \\ \rho_S & \tau_S{}^2 - \rho_S{}^2 \end{pmatrix} \tag{35}$$

Then, the transfer matrix representing the layer without interface can be computed according to the following formula, derived from Eq. (34):

$$\mathbf{M} = \tilde{\mathbf{F}}_{01}{}^{-1} \cdot \mathbf{M}_S \cdot \tilde{\mathbf{F}}_{10}{}^{-1} \tag{36}$$

By way of illustration, we can consider a typical refractive index for papers and polymers: $n = 1.5$. We have $\tilde{R}_{01} = 0.09$, $\tilde{R}'_{01} = 0.60$, $\tilde{T}_{01} = 0.91$ and $\tilde{T}'_{01} = 0.40$. $\tilde{\mathbf{F}}_{01}$ and $\tilde{\mathbf{F}}_{10}$, respectively given by Eqs. (32) and (33), can be evaluated and their inverse can be numerically computed. Eq. (36) becomes:

$$\mathbf{M} = \begin{pmatrix} 0.775 & 1.5 \\ -0.225 & 2.5 \end{pmatrix} \cdot \mathbf{M}_S \cdot \begin{pmatrix} 0.341 & 0.099 \\ -0.659 & 1.099 \end{pmatrix} \tag{37}$$

The instrinsic reflectance ρ_h and transmittance τ_h of the diffusing layer (without interface) can then be deduced from **M** using the formulas (6) and (7).

5. Case of thick nonscattering layers

The matrix model can also be used with slices of nonscattering medium, where light reflections can occur only at the interfaces. We consider in this section layers whose thickness is much larger than the coherence length of the light, i.e. where no interference can occur. The quantities *I* and *J* are incoherent, directional fluxes. The matrix representing the layer considered without interfaces is

$$\mathbf{L}(\alpha_1, d_1, \theta_1) = \begin{pmatrix} e^{\alpha_1 d_1/\cos\theta_1} & 0 \\ 0 & e^{-\alpha_1 d_1/\cos\theta_1} \end{pmatrix} \tag{38}$$

where θ_1 denotes the orientation of light in the layer, d_1 the thickness of the layer and α_1 its linear absorption coefficient which is related to the imaginary part of the refractive index, k_1, by:

$$\alpha_1 = \frac{4\pi k_1}{\lambda}. \tag{39}$$

Since according to Beer's law the term

$$t_1 = e^{-\alpha_1 d_1}, \tag{40}$$

is the transmittance of the layer at normal incidence (hereinafter called "normal transmittance"), the matrix $\mathbf{L}(\alpha_1, d_1, \theta_1)$ may also be written

$$\mathbf{L}(t_1, \theta_1) = \begin{pmatrix} t_1^{-1/\cos\theta_1} & 0 \\ 0 & t_1^{1/\cos\theta_1} \end{pmatrix}, \tag{41}$$

Regarding the interface between two media (labeled *k* and *l*), the Fresnel angular reflectance depends on the polarization of the incident flux. For a linearly polarized beam coming from medium *k* at the angle θ_k, the reflectance is denoted $R_{s,kl}(\theta_k)$ if the electric field oscillates in parallel to the incidence plane (*p*-polarization), and $R_{p,kl}(\theta_k)$ if the electric field oscillates perpendicularly to the incidence plane (*s*-polarization). The Fresnel transmittance is $T_{*kl}(\theta_k) = 1 - R_{*kl}(\theta_k)$, where symbol * denotes either *s* or *p*. For light coming from the medium *l* at the angle $\theta_l = \arcsin(n_k \sin\theta_k / n_l)$, the Fresnel reflectance is $R_{*kl}(\theta_k) = R_{*lk}(\theta_l)$ and the transmittance is $T_{*kl}(\theta_k) = T_{*lk}(\theta_l) = 1 - R_{*kl}(\theta_k)$. The transfer matrix $\mathbf{F}_{*kl}(\theta_k)$ representing the interface, defined by Eq. (4), can thus be expressed in terms of θ_k only :

$$\mathbf{F}_{*kl}(\theta_k) = \frac{1}{1 - R_{*kl}(\theta_k)} \begin{pmatrix} 1 & -R_{*kl}(\theta_k) \\ R_{*kl}(\theta_k) & 1 - 2R_{*kl}(\theta_k) \end{pmatrix} \tag{42}$$

The transfer matrix representing a stack of thick layers with different indices is the product of the transfer matrices representing the front interface (evaluated for the considered incident angle θ_0 in air), the first layer (evaluated at the angle $\theta_1 = \arcsin\left(\sin\theta_0 / n_1\right)$), the second interface (evaluated at this angle θ_1), the second layer (evaluated at the angle $\theta_2 = \arcsin\left(\sin\theta_0 / n_2\right)$), and so on… From the resulting matrix, one deduces the angular reflectances of the stack, denoted $R_{*0123\ldots N}\left(\theta_0\right)$ and $R'_{*0123\ldots N}\left(\theta_0\right)$, and their angular transmittances, $T_{*0123\ldots N}\left(\theta_0\right)$ and $T'_{*0123\ldots N}\left(\theta_0\right)$, for the considered incident angle and the considered polarization. If the incident flux is unpolarized, the reflectances and transmittances of the stack are the averages of the two corresponding polarized angular functions:

$$X_{0123\ldots N}\left(\theta_0\right) = \frac{1}{2}\left[X_{p0123\ldots N}\left(\theta_0\right) + X_{s0123\ldots N}\left(\theta_0\right)\right] \tag{43}$$

where X represents either R, R', T or T'. If furthermore the incident flux is Lambertian, the angular reflectances and transmittances are integrated over the hemisphere, thus yielding diffuse reflectances and transmittances:

$$\tilde{X}_{0123\ldots N} = \int_{\theta_0=0}^{\pi/2} X_{0123\ldots N}\left(\theta_0\right)\sin\left(2\theta_0\right)d\theta_0 \tag{44}$$

This matrix method is suitable to stacks of colored or printed films such as those studied in Ref. [25, 11, 26] where reflectance and transmittance expressions were derived from iterative methods based on geometrical series or continuous fractions. The matrix method yields the same analytical expressions by simple matrix product.

6. Case of thin films

Some nonscattering specimens may contain both thin and thick layers within which the multiple reflections should be respectively described in coherent and incoherent modes. The two types of layers may be considered successively as proposed by Centurioni [27], who uses similar matrix approach as the one presented here. It is possible to address loss of coherence due to defects or impurities, by introducing scattering in the layers [33,34] or a random parameter in the phase angle expression [28].

In the case of thin films, the quantities I and J represent the complex amplitudes of polarized electric fields. The corresponding transfer matrices are expressed in terms of the Fresnel reflectivities and transmittivities of the interfaces (different from the Fresnel angular reflectance and transmittance presented in the previous section in the case of thick layers), which depend upon polarization and propagation directions of the fields [13], and possibly upon wavelength if the indices of the media themselves depend upon wavelength.

Let us consider a flat interface between media 0 and 1 with respective refractive indices n_0 and n_1, receiving a wave from medium 0. The angle between the propagation direction and the normal of the interface is denoted θ_0. If the electric fields oscillate perpendicularly to the incidence plane (*s*-polarization), the reflectivity and transmittivity of the interface are

$$\begin{aligned} r_{s01}\left(\theta_0\right) &= \frac{n_0\cos\theta_0 - n_1\cos\theta_1}{n_0\cos\theta_0 + n_1\cos\theta_1}, \\ t_{s01}\left(\theta_0\right) &= \frac{2n_0\cos\theta_0}{n_0\cos\theta_0 + n_1\cos\theta_1}. \end{aligned} \tag{45}$$

where θ_1 denotes the angle between the propagation direction of the wave in medium 1 and the normal of the interface, satisfying $n_0 \sin\theta_0 = n_1 \sin\theta_1$. If the electric fields oscillate in the incidence plane (p-polarization), the reflectivity and transmittivity of the interface are

$$\begin{aligned} r_{p01}(\theta_0) &= \frac{n_1 \cos\theta_0 - n_0 \cos\theta_1}{n_1 \cos\theta_0 + n_0 \cos\theta_1}, \\ t_{p01}(\theta_0) &= \frac{2n_0 \cos\theta_0}{n_1 \cos\theta_0 + n_0 \cos\theta_1}. \end{aligned} \tag{46}$$

Recall that the Fresnel angular reflectances $R_{p01}(\theta_0)$ and $R_{s01}(\theta_0)$ used in the previous section in the context of single interface in incoherent mode are, for each polarization, the squared modulus of the reflectivities $r_{p01}(\theta_0)$ and $r_{s01}(\theta_0)$ [13].

When the wave comes from medium 1 at the angle θ_1 related to θ_0 by Snell's law, the reflectivity $r_{*10}(\theta_0)$ and the transmittivity $t_{*10}(\theta_0)$ for each polarization (symbol * denoting ethier *s* or *p*) are related to $r_{*01}(\theta_0)$ and $t_{*01}(\theta_0)$ according to the following equalities:

$$\begin{aligned} r_{*10}(\theta_1) &= -r_{*01}(\theta_0), \\ t_{*01}(\theta_1) &= 1 - r_{*01}(\theta_0), \\ t_{*10}(\theta_1) t_{*01}(\theta_0) &= 1 - r_{*01}^2(\theta_0). \end{aligned}$$

The transfer matrix $\mathbf{m}_{*01}$ representing the interface is similarly defined as Eq. (4) and it can be simplified as follows according to the previous relations:

$$\mathbf{m}_{*01}(\theta_0) = \frac{1}{1 - r_{*01}(\theta_0)} \begin{bmatrix} 1 & r_{*01}(\theta_0) \\ r_{*01}(\theta_0) & 1 \end{bmatrix} \tag{47}$$

Once having crossed the interface, the wave propagates at the angle θ_1 into the layer of medium 1 with thickness d_1 and undergoes a phase angle

$$\beta_1 = \frac{2\pi}{\lambda} d_1 n_1 \cos\theta_1 \tag{48}$$

The corresponding transfer matrix, $\mathbf{m_1}(d_1)$, is again defined as Eq. (4) but with zero reflectivities:

$$\mathbf{m}_1(d_1, \theta_1) = \begin{bmatrix} e^{-j\beta_1} & 0 \\ 0 & e^{j\beta_1} \end{bmatrix} \tag{49}$$

with $j = \sqrt{-1}$.

When the thin layer is absorbing, the refractive index is a complex number denoted $\hat{n}_1 = n_1 + jk_1$. The propagation angle $\hat{\theta}_1 = \arcsin(\sin\theta_0 / \hat{n}_1)$ and the phase angle

$$\hat{\beta}_1 = \beta_1 + j\gamma_1 = \frac{2\pi}{\lambda} d_1 \hat{n}_1 \cos\hat{\theta}_1 \tag{50}$$

are also complex. The matrix $\mathbf{m}(d_1, \theta_1)$ representing the thin absorbing layer is still given by Eq. (49) and can be written as the product of two matrices, one with real entries representing absorption and one with complex entries representing interferences:

$$\mathbf{m}_1(d_1, \theta_1) = \begin{bmatrix} e^{-j\hat{\beta}_1} & 0 \\ 0 & e^{j\hat{\beta}_1} \end{bmatrix} = \begin{bmatrix} e^{\gamma_1} & 0 \\ 0 & e^{-\gamma_1} \end{bmatrix} \begin{bmatrix} e^{-j\beta_1} & 0 \\ 0 & e^{j\beta_1} \end{bmatrix} \tag{51}$$

In some cases, the imaginary part of the refractive index is much lower than the real part, i.e. $k_1 \ll n_1$. Then, the complex phase angle can be written

$$\hat{\beta}_1 = \frac{2\pi}{\lambda} d_1 \left(n_1^2 \cos^2 \theta_1 - k_1^2 + 2jk_1 n_1 \right)^{1/2} \tag{52}$$

with $\theta_1 = \mathrm{Re}\left(\hat{\theta}_1\right)$. A polynomial approximation at the first order of Eq. (52) yields the same expression as Eq. (48) for β_1, and the following expression for γ_1:

$$\gamma_1 = \frac{2\pi}{\lambda} d_1 \frac{k_1}{\cos\theta_1} \tag{53}$$

Interferences can occur only if the layer is thinner than the coherence length of light, has plane and parallel surfaces, and does not scatter light. If the wave is scattered due to rough interfaces or heterogeneities in the layer, or if the thickness of the layer is too large, the coherence of light may be reduced, and even completely lost. In incoherent mode, the real part β_1 of the phase angle varies rapidly and randomly between $-\pi$ to π and can be averaged. Since the average value of the terms $e^{j\beta_1}$ and $e^{-j\beta_1}$ is 1, one has:

$$\frac{1}{2\pi} \int_{\beta_1=-\pi}^{\pi} \begin{bmatrix} e^{-j\beta_1} & 0 \\ 0 & e^{j\beta_1} \end{bmatrix} d\beta_1 = \begin{bmatrix} 1 & 0 \\ 0 & 1 \end{bmatrix}, \tag{54}$$

and Eq. (51) becomes:

$$\mathbf{m}_1(d_1, \theta_1) = \begin{bmatrix} e^{\gamma_1} & 0 \\ 0 & e^{-\gamma_1} \end{bmatrix} \tag{55}$$

with γ_1 given by Eq. (53).

The matrix approach to model the reflection and transmission of light by thin films is widely used in ellipsometry [13, 29]. For a stack of N thin films labeled 0, 1, 2,…, N and a given polarization, one obtains the transfer matrix $\mathbf{m}_{*0123\ldots N}(\theta_0)$ by multiplying the transfer matrices representing the interfaces and the layers in respect to their front-to-back position, for the considered polarization:

$$\begin{aligned} \mathbf{m}_{*0123\ldots N}(\theta_0) = \mathbf{m}_{*01}(\theta_0)\mathbf{m}_1(d_1, \theta_1)\mathbf{m}_{*12}(\theta_1)\ldots \\ \ldots\mathbf{m}_{*N-1,N}(\theta_{N-1}) \end{aligned} \tag{56}$$

The reflectivity and transmittivity of the multilayer, denoted $r_{*0123\ldots N}(\theta_0)$ and $t_{*0123\ldots N}(\theta_0)$ for each polarization $*$, are deduced from the entries of the transfer matrix according to relations (6). In order to convert them into reflectance and transmittance, one uses the Poynting complex vector [13] which relates an electric field amplitude E_* and the corresponding flux Φ_*. For the two polarization *s* and *p*, the incident fluxes are

$$\Phi_s = C\left|E_s\right|^2 \mathrm{Re}\left(\hat{n}_1 \cos\theta_1\right),$$
$$\Phi_p = C\left|E_p\right|^2 \mathrm{Re}\left(\hat{n}_1^* \cos\theta_1\right),$$

where the symbol $|x|$ denotes the modulus of the complex quantity x, y^* denotes the conjugate of the complex refractive index y, and C is a constant. The reflected fields are

$$\Phi_s = C\left|r_{s0123\ldots N}(\theta_0)E_s\right|^2 \mathrm{Re}\left(\hat{n}_1\cos\theta_1\right),$$
$$\Phi_p = C\left|r_{p0123\ldots N}(\theta_0)E_p\right|^2 \mathrm{Re}\left(\hat{n}_1^*\cos\theta_1\right),$$

and the transmitted fields are

$$\Phi_{s,t} = C\left|t_{s0123\ldots N}(\theta_0)E_s\right|^2 \mathrm{Re}\left(\hat{n}_N\cos\theta_N\right),$$
$$\Phi_{p,t} = C\left|t_{p0123\ldots N}(\theta_0)E_p\right|^2 \mathrm{Re}\left(\hat{n}_N^*\cos\theta_N\right),$$

It thus comes that the reflectance of the multilayer, ratio of the reflected to incident fluxes, is the squared modulus of the reflectivity for every polarization:

$$R_{*0123\ldots N}(\theta_0) = \left|r_{*0123\ldots N}(\theta_0)\right|^2 \tag{57}$$

and that its transmittance, ratio of the transmitted to incident fluxes, is differently expressed for the two polarizations:

$$T_{s0123\ldots N}(\theta_0) = \left|t_{s0123\ldots N}(\theta_0)\right|^2 \frac{\mathrm{Re}\left(\hat{n}_N\cos\theta_N\right)}{\mathrm{Re}\left(\hat{n}_0\cos\theta_0\right)}, \tag{58}$$

$$T_{p0123\ldots N}(\theta_0) = \left|t_{p0123\ldots N}(\theta_0)\right|^2 \frac{\mathrm{Re}\left(\hat{n}_N^*\cos\theta_N\right)}{\mathrm{Re}\left(\hat{n}_0^*\cos\theta_0\right)}. \tag{59}$$

For unpolarized incident light, the reflectance and transmittance are the average of the two polarized reflectances, respectively transmittances. If the incident light is Lambertian, these angular reflectance and transmittance expression are integrated over the hemisphere in a similar way as in Eqs. (44).

7. Combining different configurations

In the previous sections, we introduced the matrix model in three different configurations based on different properties of the light. In the configuration corresponding to thin coatings, the light is coherent, collimated and polarized. We can multiply matrices representing interfaces and layers, respectively defined by Eq. (47) and by Eq. (49). In the configuration corresponding to thick nonscattering layers, the light is incoherent, collimated and polarized. We can multiply matrices representing interfaces and layers, respectively defined by Eq. (42) and by Eq. (41), as well as transfer matrices representing thin coatings expressed in terms of their global reflectances and the transmittances defined for incoherent fluxes [see Eqs. (57) to (59)]. Lastly, in the configuration corresponding to diffusing layers, the light is incoherent, diffuse and unpolarized. We can multiply matrices representing interfaces and layers, respectively defined by Eqs. (32) and (30), as well as matrices representing nonscattering layers, stacks of nonscattering layers, stacks of thin coatings, etc., defined in terms of their reflectance and transmittance for diffuse, unpolarized fluxes by using Eqs. (43) and (44).

It is important to notice that matrices can be multiplied only when they are defined for the same configuration. It is possible to compute the reflectances and the transmittances of a multilayer component in one configuration (e.g. for coherent light), to turn them to a second configuration (e.g. for incoherent light) and to define a transfer matrix from these latters. The transfer matrix thus defined

for this second configuration can be multiplied with other matrices representing layers and interfaces defined in this same configuration. This is what we propose to illustrate in detail through an experimental example involving the three configurations, i.e. a thin silicon coating, a thick glass plate, and a diffusing background.

8. Application of the matrix method to an illustrating experience

In this experiment, two types of thin amorphous silicon deposits with respective thickness 4.8 nm and 10.8 nm have been produced on glass plates by magnetron sputtering [30]. Same deposits were produced on a first glass plate of thickness 1 mm with ground back face (Samples A) and on a second glass plate of thickness 150 µm with smooth surfaces (Samples B). The structure of the different samples is shown in Fig. 2. The complex refractive index $\hat{n}_1(\lambda) = n_1(\lambda) + jk_1(\lambda)$ of amorphous silicon measured by ellipsometry and plotted in Fig. 3 is consistent with tabulated data [31]. The refractive index n_2 of the glass is assumed to be 1.5 in the visible spectrum. In this section, labels 0, 1 and 2 are respectively attributed to air, silicon, and glass.

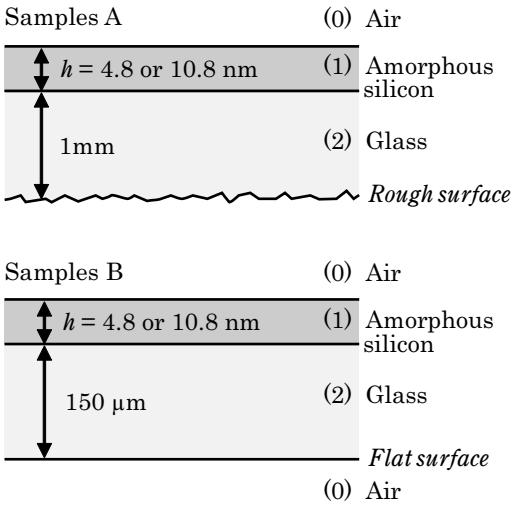

Figure 2: Description of the multilayer samples A and B.

We will first consider the thin coatings for coherent light, then for incoherent light. Then, we will consider the coatings on the glass plates for incoherent, polarized collimated flux, then for incoherent, unpolarized diffuse flux. Finally, we will consider the coated plates in front of a diffusing background.

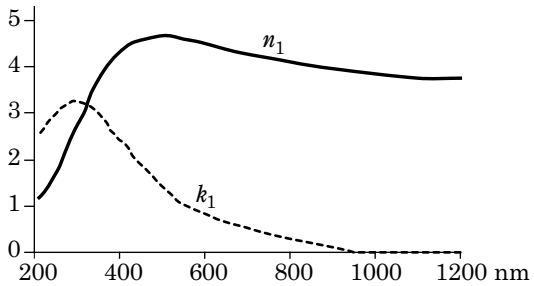

Figure 3: Real index n_1 *(solid line) and extinction coefficient* k_1 *(dashed line) of amorphous silicon.*

The spectral reflectance of samples A was measured at near-mormal incident (7° from the normal of the samples) in mode VW using the Agilent technologies™ Cary5000 spectrophotometer [32]. Since the back face of the glass plate is rough, no light is specularly reflected by this face towards the measuring instrument. Hence, the measured reflectance corresponds to the reflectance of the thin coating at 7°, $R_{012}(7°) = \left|r_{012}(7°)\right|^2$ [Eq. (57)]. Let us compute it using the matrix model according to the matrix method explained in Section 3.

We are in the configuration where the incident light is coherent, polarized and collimated. It comes at the front side with an angle θ_0. The transfer matrix representing the coating is the product of the transfer matrices representing respectively the air-silicon interface [Eq. (47)], the silicon layer itself [Eq. (51)] and the silicon-glass interface [Eq. (47)]:

$$\begin{aligned}\mathbf{m}_{*012}(\theta_0) &= \mathbf{m}_{*01}(\theta_0)\mathbf{m}_1(d_1,\theta_1)\mathbf{m}_{*12}(\theta_1)\\ &= \frac{e^{-j\hat{\beta}_1}}{(1-r_{*01})(1-r_{*12})}\begin{bmatrix}1+r_{*01}r_{*12}e^{-2j\hat{\beta}_1} & r_{*12}+r_{*01}e^{-2j\hat{\beta}_1}\\ r_{*01}+r_{*12}e^{-2j\hat{\beta}_1} & r_{*01}r_{*12}+e^{-2j\hat{\beta}_1}\end{bmatrix}\end{aligned} \tag{60}$$

with r_{*01} the reflectivity of the air-coating interface evaluated at the angle θ_0, r_{*12} the reflectivity of the coating-glass interface evaluated at the angle $\theta_1 = \mathrm{Re}\left(\arcsin\left(\sin\theta_0 / \hat{n}_1\right)\right)$, and $\hat{\beta}_1$ the phase angle given by Eq. (50). Note that all the terms in Eq. (60) depend on wavelength, included the reflectivities.

From $\mathbf{m}_{*012}(\theta_0)$, using the formulas (6), we deduce the reflectances and transmittances of the coating:

$$\begin{aligned}r_{*012}(\theta_0) &= \frac{1}{\Delta}\left(r_{*01}+r_{*12}e^{-2j\hat{\beta}_1}\right),\\ r'_{*012}(\theta_0) &= \frac{-1}{\Delta}\left(r_{*12}+r_{*01}e^{-2j\hat{\beta}_1}\right),\\ t_{*012}(\theta_0) &= \frac{1}{\Delta}(1-r_{*01})(1-r_{*12})e^{-j\hat{\beta}_1},\\ t'_{*012}(\theta_0) &= \frac{1}{\Delta}(1+r_{*01})(1+r_{*12})e^{-j\hat{\beta}_1},\end{aligned} \tag{61}$$

with

$$\Delta = 1 + r_{*01}r_{*12}e^{-2j\hat{\beta}_1}.$$

We can now consider incoherent, unpolarized collimated incident fluxes (second configuration). The corresponding reflectances and transmittances of the coating are derived from Eqs. (61) according to the relations (57) to (59), by noticing for the transmittance expressions that air and glass have real refractive indices:

$$\begin{aligned}R_{*012}(\theta_0) &= \left|r_{*012}(\theta_0)\right|^2,\\ R'_{*012}(\theta_0) &= \left|r'_{*012}(\theta_0)\right|^2,\\ T_{*012}(\theta_0) &= \left|t_{*012}(\theta_0)\right|^2 n_2\,\mathrm{Re}(\cos\theta_2)/\cos\theta_0,\\ T'_{*012}(\theta_0) &= u\cdot\left|r'_{*012}(\theta_0)\right|^2 n_2\,\mathrm{Re}(\cos\theta_2)/\cos\theta_0.\end{aligned} \tag{62}$$

The reflectance $R_{012}(7°)$ of the two Samples A that we want to predict is the average of $R_{s012}(\theta_0)$ and $R_{p012}(\theta_0)$ expressed in Eq. (62). Predicted and measured reflectances are compared in Fig. 4. They coincide fairly well, especially in the visible spectral domain (400-750 nm).

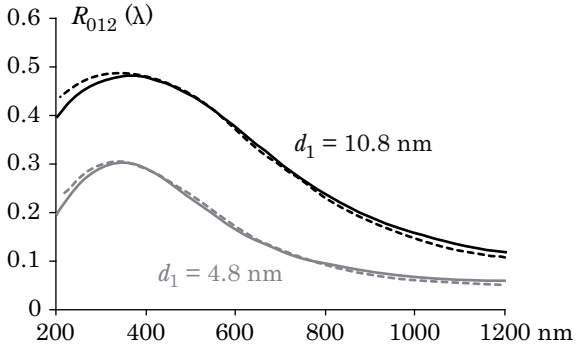

Figure 4: Predicted (dashed line) and measured (solid line) spectral reflectances of silicon coatings on 1mm thick glass plates (Samples A) at 7° from the normal.

Regarding the samples B, their reflectances and transmittances can also be predicted by the matrix method. Since the back surface of the glass plate is flat, the model must account for the specularly reflected light. Assuming that the thickness d_2 = 150 µm of the glass plate is higher than the coherence length of light, we are in the second configuration and the transfer matrix representing the glass layer is given by Eq. (41):

$$\mathbf{L}(t_2,\theta_2)=\begin{bmatrix} t_2^{-1/\cos\theta_2} & 0 \\ 0 & t_2^{1/\cos\theta_2} \end{bmatrix} \tag{63}$$

where t_2 is the normal transmittance of the glass layer in the considered spectral band, and $\theta_2=\arcsin(\sin\theta_0/n_2)$. The global transfer matrix $\mathbf{M}_{*020}(\theta_0)$ representing the glass plate without coating is the product of the following transfer matrices: the matrix $\mathbf{F}_{*02}(\theta_0)$ representing the front interface [Eq. (42)], the matrix $\mathbf{L}(t_2(\lambda),\theta_2)$ representing the glass slice [Eq. (63)] and the matrix $\mathbf{F}_{*20}(\theta_2)$ representing the back interface [also Eq. (42)]:

$$\mathbf{M}_{*020}(\theta_0)=\mathbf{F}_{*02}(\theta_0)\mathbf{L}(t_2,\theta_2)\mathbf{F}_{*20}(\theta_2) \tag{64}$$

The transmittance of the glass plate, given by inversing the top-left entry of $\mathbf{M}_{*020}(\theta_0)$, is:

$$T_{*020}(\theta_0)=\frac{\left[1-R_{*02}(\theta_0)\right]^2 t_2^{1/\cos\theta_2}}{1-R_{*02}^2(\theta_0)t_2^{2/\cos\theta_2}} \tag{65}$$

This transmittance is often measured at normal incidence. Since $R_{02}(0°)=(n_2-1)^2/(n_2+1)^2$, one has:

$$T_{020}(0°)=\frac{16n_2^2t_2}{(n_2+1)^4-(n_2-1)^4t_2^2(\lambda)}, \tag{66}$$

and therefore:

$$t_2 = \frac{\sqrt{64n_2^4 + \left(n_2^2 - 1\right)^4 T_{020}^2\left(0°\right)} - 8n_2^2}{\left(n_2 - 1\right)^4 T_{020}\left(0°\right)}. \tag{67}$$

This formula enables computing the normal transmittance of the glass slice in each spectral band as soon as the spectral transmittance of the plate is measured.

Once the coating is deposited on the glass plate, we consider the coating in place of the front air-glass interface. Hence, in the matrix product written in Eq. (64), we consider the matrix $\mathbf{M}_{*012}\left(\theta_0\right)$ representing the coating, defined from the reflectances and transmittances given by Eq. (62), in place of the matrix $\mathbf{F}_{*02}\left(\theta_0\right)$. The matrix $\mathbf{M}_{*0120}\left(\theta_0\right)$ representing the coated glass plate is therefore given by:

$$\mathbf{M}_{*0120}\left(\theta_0\right) = \mathbf{M}_{*012}\left(\theta_0\right)\mathbf{L}\left(t_2, \theta_2\right)\mathbf{F}_{*20}\left(\theta_2\right). \tag{68}$$

After computation, we obtain the following expression for the forward transmittance of the coated glass plates:

$$T_{*0120}\left(\theta_0\right) = \frac{T_{*012}\left(\theta_0\right)T_{*02}\left(\theta_0\right)t_2^{1/\cos\theta_1}}{1 - R'_{*012}\left(\theta_0\right)R_{*02}\left(\theta_0\right)t_2^{2/\cos\theta_1}}. \tag{69}$$

The term t_2 being known from Eq. (67), we can predict the transmittance of the coated plate for each wavelength, each polarization and each coating thickness. The predicted spectral transmittances for unpolarized light (average of the two polarized transmittances), are compared to the ones measured using the Cary 5000 spectrophotometer in Fig. 5. Once again, good prediction accuracy is achieved in the visible spectral domain.

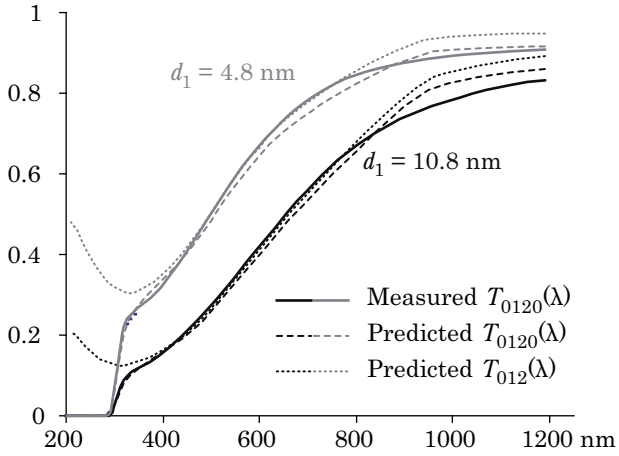

Figure 5: Predicted (dashed line) and measured (solid line) spectral transmittance at normal incidence (θ_0 = 0°) of silicon coatings on smooth glass plates of thickness 150 µm (Samples B).

Through this example, we see how the matrix method eases the derivation of reflectance and/or transmittance expressions for multilayers while using thoroughly the appropriate optical laws (coherent or incoherent modes) according to the thickness of each layer.

Taking into account the back glass-air interface, as permitted by the present method, is crucial for good accuracy of the model. Ignoring this interface would mean that the sample has the transmittance

$T_{012}(\lambda)$ instead of the transmittance $T_{0120}(\lambda)$, but we see through the spectra plotted in dotted lines in Fig. 5 that this approximation is not accurate, mainly because it does not account for the absorbance of the glass (mainly in the UV spectral domain) nor the transmittance of the back glass-air interface (thus yielding slight overestimation of the global transmittance of the samples).

It is also crucial to consider the fact that the light is coherent only in the thin coating and not in the glass plate. Considering that light remains coherent across the whole sample would predict noticeable spectral oscillations due to interferences in the glass plate which are not observed in the visible spectral domain and just perceptible in the infrared (1500-1700 nm) due to partial coherence of light in this spectral domain, as shown in Fig. 6-a. A Taylor expansion of Eq. (48) yields a first approximation of the spectral period $\Delta\lambda$ of these oscillations:

$$\Delta\lambda \approx \frac{\lambda^2}{2 d_2 n_2 \cos\theta_2}, \tag{70}$$

which seems to be in accordance with the measured oscillations, as shown in Fig. 6-b. However, it is more difficult to estimate the oscillation amplitude: the loss of coherence especially depends of the thin roughness of the interfaces [33].

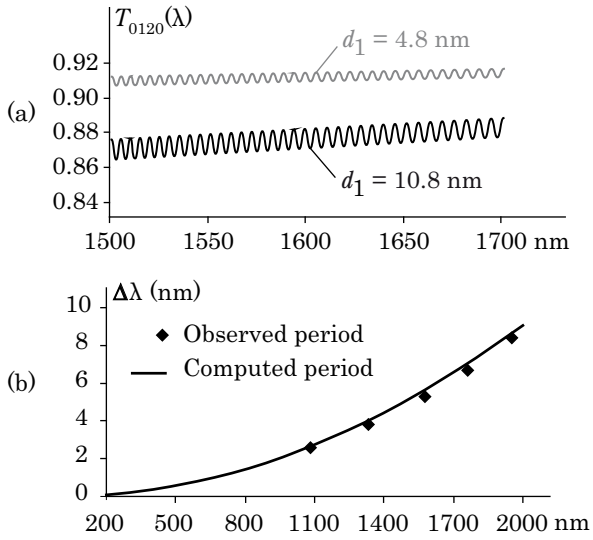

Figure 6: (a) Spectral oscillations observed in the measured spectral transmittance of Samples B in the infrared domain. (b) Spectral period Δλ of these oscillations as a function of wavelength in the infrared domain, given by Eq. (70) with d_2 *= 150 µm,* θ_2 *= 0° and* n_2 *= 1.5.*

Now that the reflectance and the transmittance of the coated glass plates (samples B) are predicted, we propose to place them in front of a Lambertian background with spectral reflectance $\rho_b(\lambda)$, and with spectral transmittance $\tau_b(\lambda)$ needed only for writing the equations. The incident flux is Lambertian and the reflected light is collected by an integrating sphere (so-called "diffuse-diffuse" measuring geometry). The plate with background can be modeled by multiplying the transfer matrix representing the coated plate [similar to Eq. (32)] and the one representing the background [similar to Eq. (30)]:

$$\frac{1}{\tilde{T}_{0120}}\begin{bmatrix} 1 & -\tilde{R}'_{0120} \\ \tilde{R}_{0120} & \tilde{T}_{0120}\tilde{T}'_{0120} - \tilde{R}_{0120}\tilde{R}'_{0120} \end{bmatrix} \cdot \frac{1}{\tau_b}\begin{pmatrix} 1 & -\rho_b \\ \rho_b & \tau_b^2 - \rho_b^2 \end{pmatrix},$$

After computation, we obtain the reflectance of the coated glass plate in front of the white tile:

$$\rho = \tilde{R}_{0120} + \frac{\tilde{T}_{0120}\tilde{T}_{0210}\rho_b}{\left(1-\tilde{R}_{0210}\rho_b\right)} \tag{71}$$

For other measuring geometries, the transfer matrix representing the glass plate should be accordingly modified. For example, in the case of the 45°:0° geometry, one needs to take into account the fact that a) the incident light crosses the plate at the angle 45° [corresponding transmittance $T_{0120}(45°)$], b) the incident light specularly reflected by the plate does not reaches the detector (reflectance 0 at the front side), c) only the light exiting at 0° reaches the detector [corresponding transmittance $T'_{0120}(0°)$]. For this geometry, the transfer representing the coated plate becomes

$$\frac{1}{T_{0120}(45°)}\begin{bmatrix} 1 & -\tilde{R}'_{0120} \\ 0 & T_{0120}(45°)T'_{0120}(0°) \end{bmatrix},$$

and the reflectance of the coated glass plate in front of the white tile becomes

$$\rho = \frac{T_{0120}(45°)T'_{0120}(0°)\rho_b}{\left(1-\tilde{R}'_{0120}\rho_b\right)} \tag{72}$$

In order to check the predictive accuracy of this formula, we measured the spectral reflectance of the coated glass plates (samples B) in front of a Spectralon white tile from Labsphere™ whose reflectance in the visible spectral domain is nearly 1, by using a Xenon light source collimated at 45° to the normal of the sample and a QE65000 spectrophotometer from Ocean Optics™ capturing light at 0°. The measured reflectance and the one predicted by Eq. (72) are compared in Fig. 7 for the two coated glass plates. The deviations between predictions and measurements is higher than in the previous step of the experiment, certainly because we considered ideal layers and did not take into account possible defects whose effect is emphasized in this stacking configuration. However, by looking at the similar shapes of the predicted and measured spectra, we can consider as positive this attempt to predict the reflectance of the specimen knowing only the thickness and refractive index of the thin silicon layer, the spectral normal transmittance and the refractive index of glass plate, and the spectral reflectance of the background. This noticeably extends our previous studies on thick films in front of diffusing background[25,26].

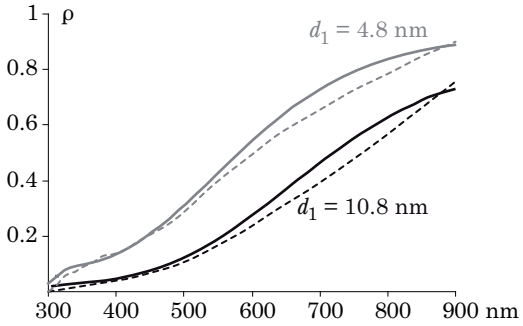

Figure 7: Measured (solid line) and predicted (dashed line) reflectance of the coated glass plates (Samples B) in front of a Lambertian white tile. Measurements are based on a 45°:0° geometry.

9. Conclusions

The method proposed in this paper should be helpful for whom wants to predict the reflectance and/or the transmittance of stratified media, of stacks of layers, or of piles of films, in which each layer can be thin or thick, but in which each medium is either nonscattering or strongly scattering (a limitation due to the two-flux-like approach underlying the matrix formalism [9]). Instead of tedious calculations of geometrical series or iterative formulas as proposed in many classical models, analytical reflectance and transmittance expressions are derived by simple matrix product where each matrix represents a layer or an interface. The matrices are defined in three different configurations, according to whether the incident light is coherent (in thin coatings), incoherent and collimated (in thick nonscattering layers), or incoherent and diffuse (in diffusing layers). The matrices representing interfaces and layers are differently defined in these three configurations and can be multiplied only if they are defined in the same configuration. However, the reflectances and transmittances of multilayer components calculated in the first configuration (coherent, polarized, collimated light) can be converted into reflectances and the transmittances in the second configuration (incoherent, polarized, collimated light), then into reflectances and the transmittances in the third configuration (incoherent, unpolarized, diffuse light). We can therefore consider hybrid specimens containing thin layers, thick nonscattering layers and diffusing layers: its global reflectance and transmittance is obtained in three steps, i.e. transfer matrices are multiplied first in the configuration (those representing the thin layers and their interfaces), then in the second configuration (the global transfer matrices representing the thin multilayers, the thick nonscattering layers and their interfaces), then in the third configuration (the global transfer matrices representing the thin-thick multilayers, the diffusing layers and their interfaces). The pedagogical example that we proposed in Section 8 illustrates these three steps and shows that good prediction accuracy can be achieved with the model.

10. Acknowledgement

This work was supported by the PHOTOFLEX project (ANR-12-NANO-0006) operated by the French National Research Agency (ANR).

11. References

1 P. Kubelka and F. Munk, “Ein Beitrag zur Optik der Farbanstriche,” *Zeitschrift für technische Physik* **12**, 593-601 (1931).

2 P. Kubelka, “New contributions to the optics of intensely light-scattering material, part I,” *J. Opt. Soc. Am.* **38**, 448–457 (1948).

3 P. Kubelka, “New contributions to the optics of intensely light-scattering materials, part II: Non homogeneous layers,” *J. Opt. Soc. Am.* **44**, 330–335 (1954).

4 G. Kortüm, Reflectance Spectroscopy, Springer Verlag (1969).

5 J.L. Saunderson, “Calculation of the color pigmented plastics,” *J. Opt. Soc. Am.* **32**, 727–736 (1942).

6 F. R. Clapper and J. A. C. Yule, The Effect of Multiple Internal Reflections on the Densities of Halftone Prints on Paper, J. Opt. Soc. Am. 43, 600-603 (1953).

7 F. C. Williams and F. R. Clapper, Multiple Internal Reflections in Photographic Color Prints, J. Opt. Soc. Am. 43, 595-597 (1953).

8 M. Hébert and R.D. Hersch, “A reflectance and transmittance model for recto-verso halftone prints,” *J. Opt. Soc. Am. A* **22**, 1952–1967 (2006).

9 M. Hébert, R. Hersch, and J.-M. Becker, "Compositional reflectance and transmittance model for multilayer specimens," *J. Opt. Soc. Am. A* **24**, 2628-2644 (2007).

10 M. Hébert, J.M. Becker, Correspondence between continuous and discrete two-flux models for reflectance and transmittance of diffusing layers, Journal of Optics A Pure and Applied Optics 10 (2008) 035006.

11 M. Hébert, J. Machizaud, "Spectral reflectance and transmittance of stacks of nonscattering films printed with halftone colors," J. Opt. Soc. Am. A 29, 2498-2508 (2012) .

12 S. Mazauric, **M. Hébert**, L. Simonot, T. Fournel, "2-flux transfer matrix model for predicting the reflectance and transmittance of duplex halftone prints," *J. Opt. Soc. Am. A* **31**, 2775-2788 (2014).

13 M. Born and E. Wolf, *Principle of Optics*, Pergamon, Oxford, 7th Edition (1999).

14 L. Simonot, M. Elias, E. Charron, "Special visual effect of art-glazes explained by the radiative transfer equation", Applied Optics 43, 2580-2587 (2004).

15. Pauli H., Eitel D. (1973) "Comparison of Different Theoretical Models of Multiple Scattering for Pigmented Media", Colour **73**, 423–426.

16 S. Chandrasekhar, *Radiative Transfert*; Dover, New-York (1960).

17. Maheu, B, Letouzan, JN, Gouesbet, G. (1984) Four-flux models to solve the scattering transfer equation in terms of Lorentz-Mie parameters. *Applied Optics* **23**, 3353–3362.

18 F. Abeles, "La théorie générale des couches minces", *Le Journal de Physique et le Radium* **11**, 307–310 (1950).

19 Emmel, P. "Physical models for color prediction", *in* Sharma, G, Bala, R. (2003) *Digital Color Imaging Handbook,* CRC Press.

20 V. Reillon · S. Berthier · C. Andraud, "Optical properties of lustred ceramics: complete modeling of the actual structure " Appl Phys A **100**, 901–910 (2010).

21 N. Destouches, N. Crespo-Monteiro, T. Epicier, Y. Lefkir, F. Vocanson, S. Reynaud, R. Charrière, M. Hébert, "Permanent dichroic coloring of surfaces by laser-induced formation of chain-like self-organized silver nanoparticles within crystalline titania films", Conf. Synthesis and Photonics of Nanoscale Materials X, Proc. of SPIE Vol. 8609-860905 (2013).

22 G. Stokes, "On the intensity of light reflected from or transmitted through a pile of plates". In: Mathematical and Physical Papers of Sir George Stokes, IV. Cambridge Univ. Press, London, 145–156 (1904).

23 G. Strang, *Applied Mathematics*, MIT Press, 1986.

24 D. B. Judd, "Fresnel Reflection of Diffusely Incident Light," *J. Res. Natl. Bur. Stand.* **29**, 329–332 (1942).

25 L. Simonot, M. Hébert, R. Hersch, "Extension of the Williams-Clapper model to stacked nondiffusing colored layers with different refractive indices," *J. Opt. Soc. Am. A* **23**, 1432-1441 (2006).

26 M. Hébert, R. Hersch, L. Simonot, "Spectral prediction model for piles of nonscattering sheets", *J. Opt. Soc. Am. A* **25** 2066-2077 (2008) .

27 E. Centurioni, Generalized matrix method for calculation of internal light energy flux in mixed coherent and incoherent multilayers, Applied Optics 44 (2005) 7532-7539.

28 M.C. Troparevsky, A.S. Sabau, A.R. Lupini, Z. Zhang, transfer-matrix formalism for the calculation of optical response in multilayer systems: from coherent to incoherent interference, Optics express 18 (2010) 24715-24721.

29 R.M. Azzam, N.M. Bashara, *Ellipsometry and Polarized Light,* North-Holland (1977).

30 L. Simonot, D. Babonneau, S. Camelio, D. Lantiat, P. Guérin, B. Lamongie, V. Antad, In-situ optical spectroscopy during deposition of Ag:Si3N4 nanocomposite films by magnetron sputtering, Thin Solid Films 518 (2010) 2637-2643.

31 E.D. Palik, *Handbbok of Optical Constants*, New York, Academic (1985).

32 J. Strong, *Procedures in experimental physics*, Prentice-Hall, Inc, (1938).

33 C. C. Katsidis and D. I. Siapkas, "General Transfer-Matrix Method for Optical Multilayer Systems with Coherent, Partially Coherent, and Incoherent Interference," Appl. Opt. 41, 3978-3987 (2002).

34 C. L. Mitsas and D. I. Siapkas, "Generalized matrix method for analysis of coherent and incoherent reflectance and transmittance of multilayer structures with rough surfaces, interfaces, and finite substrates," Appl. Opt. 34, 1678-1683 (1995).